The Response of Small Photovoltaic Detectors to Uniform Radiation

JOSEPH SHAPPIR, MEMBER, IEEE, AND AVINOAM KOLODNY

Abstract—The short-circuit photocurrent of a small photodiode under uniform illumination is discussed for the case of diffusion length larger than the absorption depth. Lateral response, resulting from carrier diffusion in the substrate near the photodiode, is taken into account. Numerical results of a two-dimensional analysis are presented and compared to one-dimensional approximations. Effects of various parameters, such as surface recombination velocity and excess carrier lifetime on the lateral response are discussed.

I. INTRODUCTION

THE PHOTOSENSITIVITY of a small photodiode under uniform illumination involves the solution of a two-dimensional diffusion equation for minority carriers, which is often encountered in modeling and analysis of semiconductor devices [1]–[5]. Similar problems have been considered in the analysis of photosensitive devices, when only a part of the device area is illuminated, or when a small device occupies a fraction of a larger illuminated area [3]–[9].

Analytical solutions to the diffusion equation in two dimensions are not easily obtained and in some cases may not be convenient for physical interpretation. In many cases a simplified one-dimensional model is assumed, which gives a better insight into the problem and may be used conveniently for design purposes [9]–[12]. For exact solutions of the problem, numerical methods are called for.

In the present study, we use both approaches, and analyse the results of a computer simulation in light of the simple one-dimensional solutions.

The device considered is a p^+-n mesa-structure photodiode of small dimensions, uniformly illuminated. The diode short-circuit current in the steady-state comprises three components:

1) I_{sc}—current resulting from carrier generation in the junction space-charge region.

2) I_P—current resulting from generated electrons in the p-type region, which reach the junction by diffusion.

3) I_N—current resulting from generated holes in the n-type bulk all around and below the device, which reach the junction by diffusion.

In the case where the absorption depth is larger than the total width of the p-type region and the underlying depletion region, the third current component I_N is the most significant in magnitude. As will be shown, this current is

greatly affected by lateral diffusion of minority carriers from the illuminated periphery of the diode towards the junction. This effect is pronounced when the lateral dimensions of the device and the minority carrier diffusion length are of the same orders of magnitude. This diffusion current—hereafter referred to as "lateral current"—is collected by the junction in addition to photogenerated current from the underlying N region. The lateral current increases the effective photosensitive area of the device, thus affecting spatial resolution which plays an important role in imaging systems.

The life of a photogenerated hole within the diode periphery may terminate by collection in the junction, by recombination in the bulk, or by surface-recombination. Since normally the radiation is absorbed close to the semiconductor surface, it is expected that surface-recombination velocity should have a strong influence on the lateral current.

II. DEVICE STRUCTURE AND PROBLEM FORMULATION

Fig. 1 shows the stripe-geometry mesa-structure to be considered. As a matter of convenience, the lower edge of the space-charge layer is assumed to coincide with the surrounding crystal surface.

Using the continuity equation for holes, and assuming that the hole-current in the bulk is due to diffusion only, we obtain the diffusion-equation for steady state:

$$\nabla^2 \hat{p} - \frac{\hat{p}}{L_p^2} = \frac{G_L(x,y,z)}{D_p} \tag{1}$$

where $\hat{p}$ denotes excess hole concentration, D_p, τ_p, and $L_p = (D_p \tau_p)^{1/2}$ are diffusion coefficient, lifetime, and diffusion length of holes in the n-type bulk, respectively, and $-G_L$ is the optical generation rate which is related to the incident photon flux density F_0.

Assuming unity quantum efficiency of the optical excitation process, we may write:

$$G_L(x,y,z)$$
$$= \begin{cases} -\alpha(F_0 e^{-\alpha x_0})e^{-\alpha x}, & |y| \leq y_m \text{ (region I)} \\ -\alpha F_0 e^{-\alpha x}, & |y| > y_m \text{ (region II)} \end{cases} \tag{2}$$

where α denotes the absorption coefficient at a given wavelength λ. Regions I and II are defined in Fig. 1, and they differ by the amount of photons absorbed in the mesa of height x_0.
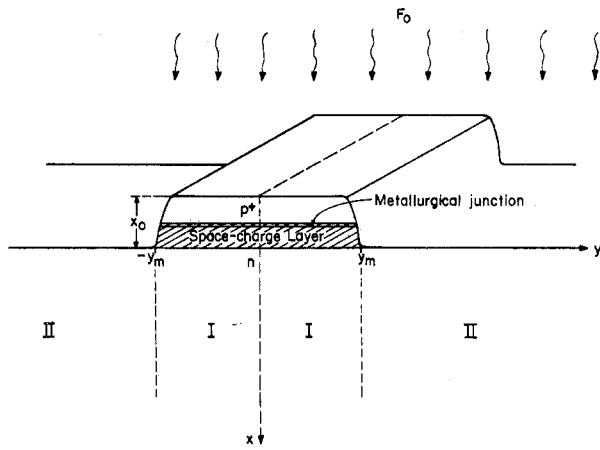
Fig. 1. Schematic device structure of stripe geometry.

Since there are no changes along the z direction, (1) may be reduced to the two-dimensional problem:

$$\frac{\partial^2 \hat{p}}{\partial x^2} + \frac{\partial^2 p}{\partial y^2} - \frac{\hat{p}}{L_p^2}$$

$$= \begin{cases} -(\alpha F_0 e^{-\alpha x_0}/D_p)e^{-\alpha x} & \text{(region I)} \\ -(\alpha F_0/D_p)e^{-\alpha x} & \text{(region II).} \end{cases} \quad (3)$$

From symmetry considerations, it suffices to find the solution in the right half of the xy plane.

The boundary conditions for (3) are

$$\hat{p}(0,y) = 0,$$

$-y_m \leq y \leq y_m$ (collection by short-circuited junction)

$$(4)$$

$$D_p \frac{\partial \hat{p}}{\partial x}\bigg|_{x=0} = s \cdot \hat{p}(0,y),$$

$$|y| > y_m \text{ (surface recombination)} \quad (5)$$

$$\hat{p}(x \to \infty, y) = 0 \quad \text{(equilibrium deep in the bulk)} \quad (6)$$

$$\frac{\partial \hat{p}}{\partial y}\bigg|_{y=0} = 0 \quad \text{(symmetry).} \quad (7)$$

In the above, s denotes the surface-recombination velocity.

Far away from the mesa, we may assume that the solution is independent of y so that (3) reduces to a one-dimensional problem, the solution for which (to be derived in the next section) may be used as a boundary condition:

$$\hat{p}(x,y \to \infty) = \frac{F_0 \alpha}{D_p[\alpha^2 - (1/L_p^2)]}$$

$$\cdot \left[\frac{D_p \alpha + s}{\sqrt{(D_p/\tau_p)} + s} e^{-(x/L_p)} - e^{-\alpha x} \right]. \quad (8)$$

Equation (3) as well as the boundary conditions are linear. Thus the general solution for radiation in any spectral range and intensity is constructed by superposition of monochromatic solutions. We therefore limit our treatment to monochromatic excitation.

The current reaching the junction by diffusion of holes in the n-region may be computed from the solution of (3) as

$$I_{\text{col}} = -q D_p \int_0^{y_m} \frac{\partial \hat{p}}{\partial x}\bigg|_{x=0} dy. \quad (9)$$

I_{col} is the total current per unit length in the z direction, collected by half of the infinitely long device depicted in Fig. 1.

III. ONE-DIMENSIONAL APPROXIMATIONS

If one assumes $(\partial^2 \hat{p}/\partial y^2) = 0$, an assumption which is valid far away from the mesa, and under the middle of the mesa in some cases (i.e., if y_m is large enough), one obtains from (3) the ordinary differential equations:

$$\frac{\partial^2 \hat{p}}{\partial x^2} - \frac{\hat{p}}{L_p^2} = -\frac{\alpha F_0 e^{-\alpha x_0}}{D_p} e^{-\alpha x},$$

$$y = 0 \text{ (under the middle of the mesa)} \quad (10a)$$

$$\frac{\partial^2 \hat{p}}{x^2} - \frac{\hat{p}}{L_p^2} = -\frac{\alpha F_0}{D_p} e^{-\alpha x}, \quad y \to \infty \text{ (far away).} \quad (10b)$$

Boundary conditions for (10a) are (4) and (6). Boundary conditions for (10b) are (5) and (6).

The respective solutions for (10a) and (10b) are

$$\hat{p}(x,0) = \frac{F_0 \alpha e^{-\alpha x_0}}{D_p[\alpha^2 - (1/L_p^2)]} [e^{-(x/L_p)} - e^{-\alpha x}] \quad (11a)$$

$$\hat{p}(x,\infty) = \frac{F_0 \alpha}{D_p[\alpha^2 - (1/L_p^2)]}$$

$$\cdot \left[\frac{D\alpha + s}{\sqrt{(D_p/\tau_p)} + s} e^{-(x/L_p)} - e^{-\alpha x} \right]$$

$$\triangleq \frac{F_0 \alpha}{D_p[\alpha^2 - (1/L_p^2)]} b(x). \quad (11b)$$

The function $b(x)$, defined by the term in brackets, which describes the behavior of the excess hole profile with varying depth far away from the mesa, is plotted in Fig. 2 for several values of s. All the values of the parameters used subsequently are given in Tables I and II and apply to the special case of an InSb photovoltaic diode operated at 77 K, viewing a 2π steradian 300 K background. For simplicity we have assumed that the total background is absorbed as if it were monochromatic light of wavelength 4.5×10^{-4} cm.

It is clearly seen that (11b) coincides with (11a) for $s \to \infty$, and $x_0 \to 0$. Thus, for a thin-mesa device with severe surface recombination, there is no lateral variation in $\hat{p}$, and there is no lateral diffusion current. The total diffusion current collected by the junction may then be computed by substituting (11a) in (9):

$|I_{\text{col}}|$ one-dimensional

$$= q D_p y_m \frac{\alpha F_0 e^{-\alpha x_0}}{D_p[\alpha^2 - (1/L_p^2)]} \left[-\frac{1}{L_p} + \alpha \right]$$

$$= q y_m F_0 e^{-\alpha x_0} \frac{\alpha}{\alpha + (1/L_p)}. \quad (12)$$
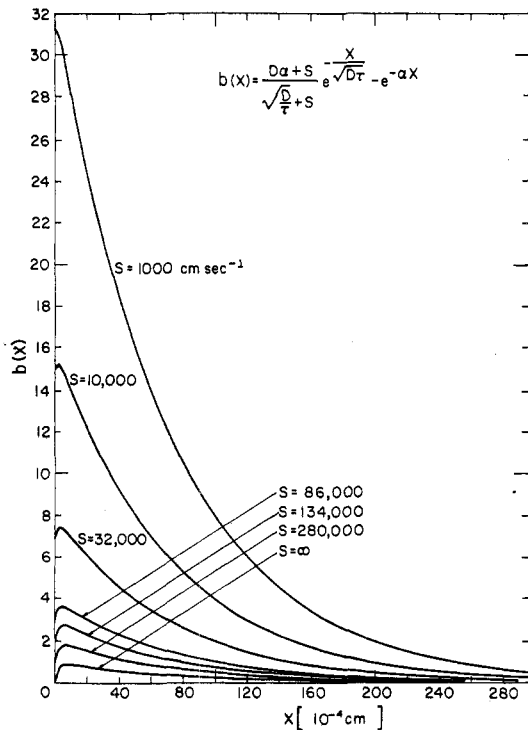
Fig. 2. Excess minority carrier profiles in the one-dimensional case with various values of surface-recombination velocity s.

TABLE I
Physical Parameters for InSb [13] at 77 K

Symbol	Parameter	Value
τ_p	Hole lifetime	0.8×10^{-6} sec
D_p	Hole diffusion coefficient	66 cm$^2 \cdot$ sec^{-1}
L_p	Hole diffusion length	72.7×10^{-4} cm
α	Absorption coefficient	4500 cm^{-1}
α^{-1}	Absorption depth	2.22×10^{-4} cm

TABLE II
Physical and Geometrical Parameters Used in the Numerical Calculations

Symbol	Parameter	Value
τ_p	Hole lifetime	0.8×10^{-6} sec, 0.8×10^{-7} sec
α	Absorption coefficient	4500 cm^{-1}, 2250 cm^{-1}
x_0	Mesa Height	1.1×10^{-4} cm, 1.5×10^{-4} cm
s	Surface recombination velocity	$0 \div 10^{6}$ cm·sec^{-1}
y_m	Half mesa width	2.5×10^{-3}cm, 5×10^{-3}cm, 1×10^{-2}cm
F_0	Photon flux density	2×10^{16} cm^{-2}·sec^{-1}

Equation (12) is hereafter referred to as "the one-dimensional approximation."

For finite surface-recombination velocity the collected photocurrent increases due to lateral diffusion of photocarriers to the p-n junction.
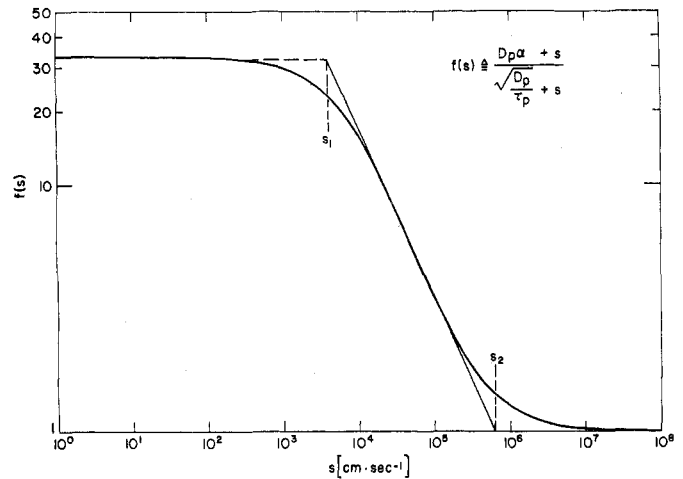
Fig. 3. Function $f(s)$ of the one-dimensional solution.
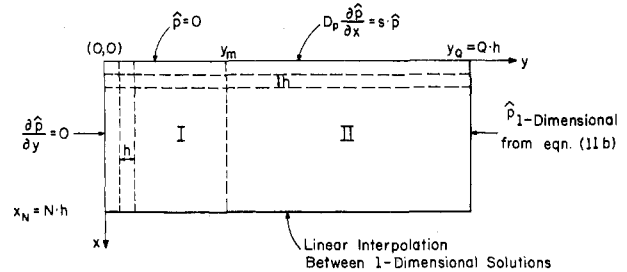
Fig. 4. Definition of the region and the boundary conditions for numerical solution of the continuity equation.

We proceed to examine the departure of the actual behavior of the device from the one-dimensional approximation as given by (12) and its dependence on certain parameters such as x_0, s, and y_m.

We observe that (11b) is the difference of two exponentials with characteristic constants L_p (diffusion length) and α^{-1} (absorption length), where α^{-1} is much smaller than L_p for the case of n-type InSb. The amplitudes of the exponentials are related by the factor:

$$f(s) \triangleq \frac{D_p\alpha + s}{\sqrt{(D_p/\tau_p)} + s}. \tag{13}$$

Graphical description of $f(s)$ is given in Fig. 3, from which we observe that there are two critical values of s, and we may expect a gradual change from a negligible lateral effect corresponding to $s > s_2$—allowing the use of (12)—to some maximum lateral effect corresponding to $s < s_1$. The values of s_1 and s_2 are close to $(D_p \cdot \tau_p^{-1})^{1/2}$ and $D_p \cdot \alpha$, respectively.

In the next sections, we check these hypotheses by solving (3) numerically, and observing the diffusion currents from the slopes of the solution for excess minority carrier concentrations.

IV. NUMERICAL SOLUTION

First, we confine ourselves to a finite portion of the xy plane, as shown in Fig. 4, and define a uniform grid of discrete points with spacing h. On the new boundaries thus

formed—a few diffusion lengths far and below the junction—we take approximations based on the one-dimensional solutions instead of the true conditions at infinity.

Next, we replace (3), using finite-differences [14]–[16],
by

$$P_{l+1,m} + P_{l,m+1} + P_{l-1,m} + P_{l,m-1} - \left(4 + \frac{h^2}{L_p^2}\right) P_{l,m}$$

$$= \begin{cases} -\dfrac{h^2 \alpha F_0 e^{-\alpha x_0}}{D_p} e^{-\alpha l \cdot h} & \text{(region I)} \\[2mm] -\dfrac{h^2 \alpha F_0}{D_p} e^{-\alpha l \cdot h} & \text{(region II).} \end{cases} \quad (14)$$

Writing (14) for $l = 0,1,\cdots,N$ and $m = 0,1,\cdots,Q$, we obtain a system of linear equations with a matrix of unknowns $P_{l,m}$. This system has a unique solution, which represents a sampling of the function $\hat{p}(x,y)$. The system is too large to be solved explicitly, so an implicit block-iterative alternating-directions method is employed, which updates $P_{l,m}$ along rows and columns, each step involving the solution of a tridiagonal system by the Thomas [16] algorithm.

Now, by numerical differentiation we get the diffusion current densities, and by integrating current density along the upper boundary of region I we compute the total current collected by the junction. All the results are per unit stripe length of one side of the device shown in Fig. 1.

A computer program to perform the above operations was executed using various sets of parameters given in Tables I and II. Numerical results and discussions are given in the next sections.

V. NUMERICAL RESULTS

The excess hole concentration in a part of the n-region near the mesa edge is illustrated in Fig. 5 for low, medium, and high surface-recombination velocities. One should note the marked decrease in excess carrier concentration as s increases and the large gradient of $\hat{p}$ close to the mesa edge. Also shown in Fig. 5 are the diffusion flow lines, and the lines separating the flow lines terminating in the junction, the surface, and the bulk. It is observed that not all the photocarriers which diffuse from region II to region I (as defined in Fig. 1) contribute to the collected current, since some of them move away from the junction into the bulk where they recombine with majority carriers. As can be seen, most of the lateral diffusion current is collected near the mesa edge. The total collected photocurrent was calculated from (9) for various values of the y_m, s, τ_p, α, and x_0. For comparison, the one-dimensional approximation, corresponding to $s \to \infty$, was calculated from (12). Normalized results are shown graphically in Fig. 6.

VI. DISCUSSION

A. Effect of Surface Recombination

The asymptotic behavior of the collected current, depicted in Fig. 6, is similar to the behavior of $f(s)$ in Fig. 3. A plot of I_{col} against $f(s)$, given in Fig. 7, shows that I_{col} is

(a)

(b)

(c)
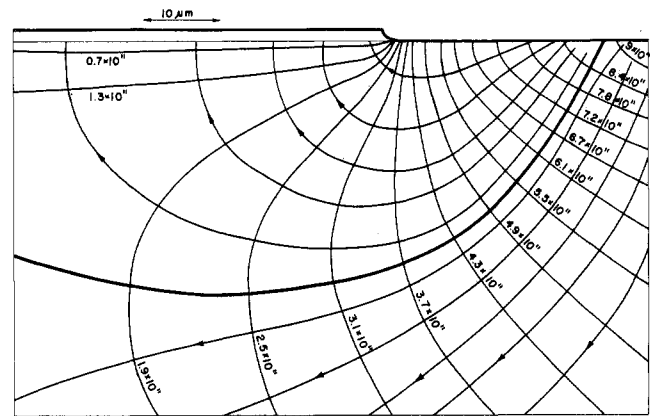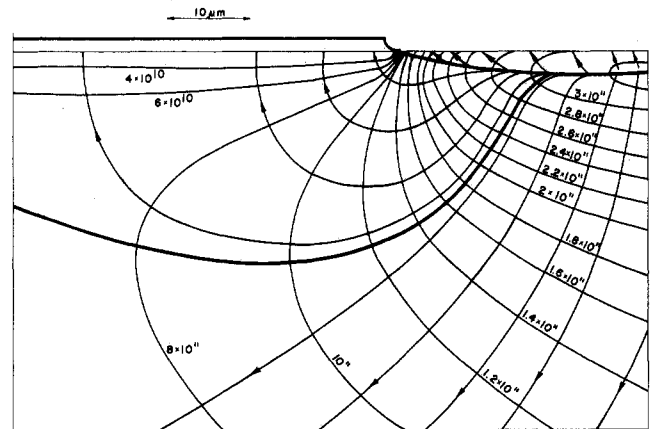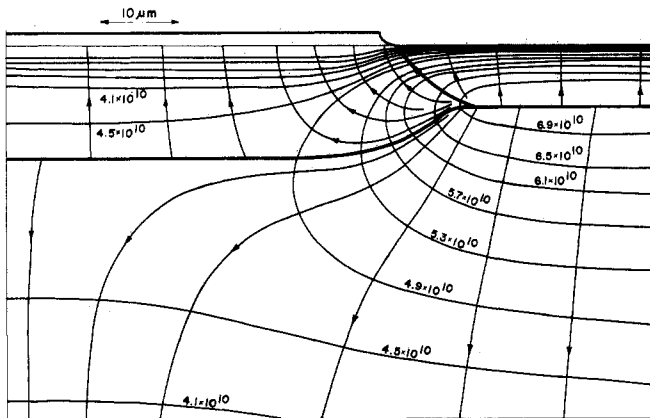
Fig. 5.   Equi-concentration curves and flow lines near the mesa edge, for $x_0 = 1.1 \times 10^{-4}$ cm and $y_m = 50 \times 10^{-4}$ cm. (a) $s = 0$, response is 62 percent higher than the one-dimensional approximation. (b) $s = 3 \times 10^4$ cm·s^{-1}, response is 13 percent higher than the one-dimensional approximation. (c) $s = 10^6$ cm·s^{-1}, response is practically equal to the one-dimensional case.

almost linearly dependent on $f(s)$ and may be approximately described by a relation of the form

$$I_{col} = I_0 + A \cdot [f(s) - 1] \triangleq I_V + I_L \quad (15)$$

which may be interpreted as the sum of a constant *vertical* current I_0 and a *lateral* current proportional to $[f(s) - 1]$. The parameters I_0 and A are dependent on device geometry. This lateral current may be modeled by assuming that the excess-holes profile changes gradually along the lateral
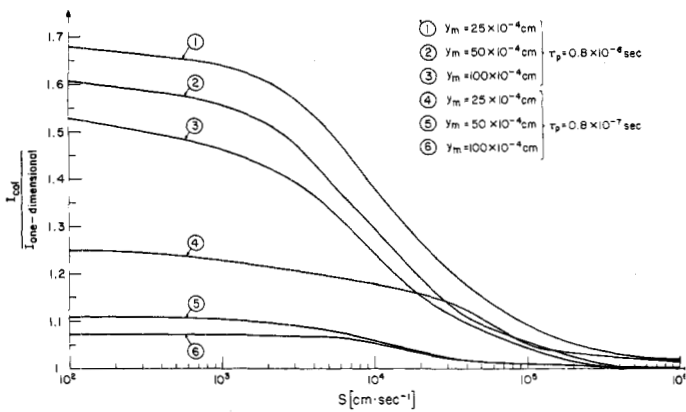
Fig. 6. Total normalized collected current as function of surface-recombination velocity for several values of τ_p and y_m.
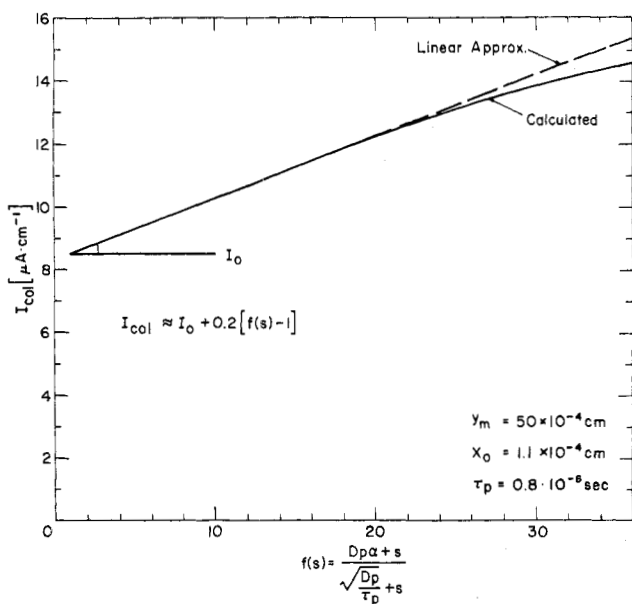
Fig. 7. Total collected current I_{col} versus $f(s)$ including linear approximation.

direction, from the one-dimensional profile of (11b) under the mesa to the profile of (11a) far away. However, such modeling ignores the detailed two-dimensional flow.

B. Effect of Mesa Width

According to the approximate model proposed above, it might be expected that the vertical current I_0 would be proportional to the mesa width y_m, and the lateral current would be independent of y_m.

However, it was found that I_L is smaller in a smaller device. In fact, the total current passing from region II to region I was calculated from computer results, and was found to be almost independent of y_m, but a larger part of it goes to bulk-recombination as y_m decreases.

C. Effects of Minority-Carrier Lifetime

The one-dimensional approximation to the collected current is fairly insensitive to variation in holes' lifetime τ_p, since absorption depth α^{-1} remains much smaller than diffusion length $L_p = (D_p \tau_p)^{1/2}$ even for reduced lifetimes.

Hence most of the photogenerated carriers below the junction are collected (by (12), the collected fraction is $L_p/(L_p + \alpha^{-1})$). The lateral diffusion current reaching the junction is much dependent on L_p, which is governed by τ_p. From Fig. 6 it may be concluded that the combination of τ_p and s determines the significance of lateral response to the total collected current.

D. Effect of Mesa Height

From computer solutions for practical mesa heights x_0 (and a hypothetical height $x_0 = 0$ too) it was concluded that the lateral response is fairly insensitive to variations in x_0, while the differences in I_{col} due to absorption in the mesa of height x_0 may be calculated from the one-dimensional approximation.

E. Effect of Absorption Coefficient

The absorption depths α^{-1} corresponding to all the detectable wavelengths in InSb are much smaller than the diffusion length L_p, and so there is no significant change in the lateral response for different wavelengths. The differences in I_{col} due to different absorption in the mesa may be calculated from the one-dimensional approximation.

VII. CONCLUSIONS

Whenever the minority carrier diffusion length is of the same order of magnitude as the photodiode dimensions, lateral contribution to the photosensitivity cannot be ignored. This is especially important in the case of imaging arrays where the spatial distribution of the absorbed radiation must be sensed accurately in order to obtain the correct image. Since normally most of the radiation is absorbed close to the surface of the semiconductor it was found, as expected, that the surface recombination velocity will significantly affect the lateral response. The maximum lateral response is obtained for surface recombination velocity $s < (D_p \tau_p^{-1})^{1/2}$ and practically no lateral response should be observed for $s > D_p \cdot \alpha$. This is true of course only for the case that $D_p \alpha/(D_p \tau_p^{-1})^{1/2} = L_p \alpha > 1$, i.e. the diffusion length of the minority carriers is larger than the absorption depth of the radiation.

REFERENCES

[1] D. Fulkerson, "A two-dimensional model for the calculation of common emitter current gains of lateral p-n-p transistors," *Solid-State Electronics*, vol. 11, pp. 821–826, 1968.
[2] D. Seltz and I. Kidron, "A two-dimensional model for the lateral p-n-p transistor," *IEEE Trans. Electron Devices*, vol. ED-21, pp. 587–592, 1974.
[3] M. K. Mukherjee *et al.*, "Two-dimensional analysis for response of a photo diode array," *Solid-State Electronics*, vol. 18, pp. 716–718, 1975.
[4] M. H. Crowell and E. F. Labuda, "The silicon diode array camera tube," *Bell Syst. Tech. J.*, vol. 48, p. 1481, 1969.
[5] M. Stark, private communication.

[6] G. Lucovsky and R. B. Emmons, "Lateral effects in high-speed photodiodes," *IEEE Trans. Electron Devices*, vol. ED-12, p. 5, 1965.

[7] G. Lucovsky, "Photoeffects in nonuniformly irradiated p-n junctions," *J. Appl. Phys.*, vol. 31, p. 1088, 1960.

[8] S. Deb *et al.*, "Response of a partially illuminated photovoltaic p-n junction cell," *Int. J. Electron.*, vol. 21, p. 89, 1966.

[9] T. M. Buck *et al.*, "Influence of bulk and surface properties on image sensing silicon diode arrays," *Bell Syst. Tech. J.*, vol. 47, p. 1827, 1968.

[10] S. Chou, "An investigation of lateral transistors," *Solid-State Electronics*, vol. 14, pp. 811–826, 1971.

[11] I. Kidron, "Integrated circuit model for lateral p-n-p transistors

including isolation junction interactions," *Int. J. Electronics*, vol. 31, pp. 421–440, 1971.

[12] M. K. Mukherjee, "The spectral response characteristics of a Cu_2S-CdS photovoltaic cell," *IEEE Trans. Electron Devices*, vol. 21, p. 379, 1974.

[13] R. A. Laff and H. Y. Fan, "Carrier lifetime in Indium Antimonide," *Phys. Rev.*, vol. 121, p. 53, 1961.

[14] A. R. Mitchell, *Computational Methods in Partial Differential Equations*. New York: Wiley, 1969.

[15] W. Ames, *Numerical Methods in Partial Differential Equations.* Nelson, 1969.

[16] J. Westlake, *A Handbook of Numerical Matrix Inversion and Solution of Linear Equations.* New York: Wiley, 1968, p. 34.

Nonvolatile Static Read/Write Memory Cell Using CMNOS Structure

SUSUMU KOIKE

Abstract—A new type of nonvolatile static read/write memory cell constructed with three MOS transistors and one MNOS transistor is proposed. The MNOS transistor and one of the MOS transistors involved are complementary combined to offer binary states in the Λ-shaped *I–V* curve for memory operation under normal power supply. Upon power failure, the MNOS transistor acts as a back-up element for nonvolatility. The new cell is characterized by advantageous features such as small cell size, simple peripheral circuit, operation with a unipolar power supply and low standby power consumption.

I. INTRODUCTION

STUDIES OF MNOS transistors have attracted much interest in the field of nonvolatile semiconductor memory devices [1], especially towards nonvolatile read/write memories (NVRWM) in these several years. However, the applications have been limited so far only to programmable read-only memories (PROM) [2], because of the slow speed (1 ~ 10 ms) in writing/erasing operation and the profound degradation of memory retention after frequent writing/erasing cycles (10^5 ~ 10^8).

Recent development by Saito *et al.* [3] has offered the first NVRWM, of which unit cell consists of eight MOS transistors for static read/write flip-flop operation and two MNOS transistors as a back-up element.

This paper proposes a new type of nonvolatile static read/write memory cell constructed with three MOS transistors and one MNOS transistor. The proposed cell

is advantageous over the above device in respects of small cell size, simple peripheral circuit, operation with unipolar power supplies, and low standby power consumption. The operation principle of the new cell is based upon an extention of the CMNOS device which we reported as a nonvolatile PROM cell in the previous paper [4].

In the following sections, the structure and operation principle of the present cell will be presented together with some preliminary experimental results.

II. CELL OPERATION

Fig. 1 shows a basic circuit configuration of the proposed cell. An n-channel MNOS transistor F_1, a p-channel depletion-mode MOS transistor F_2, and a diode are connected in series. The gate electrodes of F_1 and F_2 are connected to the drain electrodes of F_2 and F_1, respectively. An enhancement-mode p-channel MOS transistor F_3 is used as a load. The node T_1 is connected to the digit line D through a word selection transistor F_4 of enhancement mode. A common line L is used to apply a negative pulse for obtaining the nonvolatility.

The operation under normal power supply is not the same as that of the CMNOS PROM proposed [4] by the present author in spite of the similar structure. In the case of the CMNOS PROM device, the Λ-shaped *I–V* characteristic between T_1 and T_2 terminals, as shown in the curve (a) of Fig. 2, is utilized as the memorized "1" state only. In the present NVRWM cell, however, the Λ-shaped *I–V* characteristic is used as a bistable element which enables [6], [7] the static read/write operation under the normal